Defined Conditions for Differentiation of Functional Retinal Ganglion Cells From Human Pluripotent Stem Cells

Junwon Lee,[1–3] Sang-Hwi Choi,[1,3] Young-Beom Kim,[4] Ikhyun Jun,[2] Jin Jea Sung,[1,3] Dongjin R. Lee,[1,3] Yang In Kim,[4] Myung Soo Cho,[5] Suk Ho Byeon,[2] Dae-Sung Kim,[6] and Dong-Wook Kim[1,3]

[1]Department of Physiology, Yonsei University College of Medicine, Seoul, South Korea
[2]Department of Ophthalmology, Institute of Vision Research, Yonsei University College of Medicine, Seoul, South Korea
[3]Brain Korea 21 Plus Project for Medical Science, Yonsei University College of Medicine, Seoul, South Korea
[4]Department of Physiology, Korea University College of Medicine, Seoul, South Korea
[5]S.Biomedics Co., Ltd., Seoul, South Korea
[6]Department of Biotechnology, Brain Korea 21 Plus Project for Biotechnology, Korea University, Seoul, South Korea

Correspondence: Dong-Wook Kim, Department of Physiology, Yonsei University College of Medicine, 50-1 Yonsei-ro, Seodaemun-gu, Seoul 03722, South Korea; dwkim2@yuhs.ac.
Dae-Sung Kim, Department of Biotechnology, Korea University, 145 Anam-ro, Seongbuk-gu, Seoul 02841, South Korea; sonnet10@korea.ac.kr.

JL and S-HC contributed equally to the work presented here and should therefore be regarded as equivalent authors.

Submitted: November 18, 2017
Accepted: May 8, 2018

Citation: Lee J, Choi S-H, Kim Y-B, et al. Defined conditions for differentiation of functional retinal ganglion cells from human pluripotent stem cells. *Invest Ophthalmol Vis Sci*. 2018;59:3531–3542. https://doi.org/10.1167/iovs.17-23439

Purpose. We aimed to establish an efficient method for retinal ganglion cell (RGC) differentiation from human pluripotent stem cells (hPSCs) using defined factors.

Methods. To define the contribution of specific signal pathways to RGC development and optimize the differentiation of hPSCs toward RGCs, we examined RGC differentiation in three stages: (1) eye field progenitors expressing the eye field transcription factors (EFTFs), (2) RGC progenitors expressing MATH5, and (3) RGCs expressing BRN3B and ISLET1. By monitoring the condition that elicited the highest yield of cells expressing stage-specific markers, we determined the optimal concentrations and combinations of signaling pathways required for efficient generation of RGCs from hPSCs.

Results. Precise modulation of signaling pathways, including Wnt, insulin growth factor-1, and fibroblast growth factor, in combination with mechanical isolation of neural rosette cell clusters significantly enriched RX and PAX6 double-positive eye field progenitors from hPSCs by day 12. Furthermore, Notch signal inhibition facilitated differentiation into MATH5-positive progenitors at 90% efficiency by day 20, and these cells further differentiated to BRN3B and ISLET1 double-positive RGCs at 45% efficiency by day 40. RGCs differentiated via this method were functional as exemplified by their ability to generate action potentials, express microfilament components on neuronal processes, and exhibit axonal transportation of mitochondria.

Conclusions. This protocol offers highly defined culture conditions for RGC differentiation from hPSCs and in vitro disease model and cell source for transplantation for diseases related to RGCs.

Keywords: human pluripotent stem cells, induced pluripotent stem cells, retinal ganglion cells, defined factors, differentiation

Retinal ganglion cells (RGCs) transmit the visual information processed by retinal cells, such as photoreceptors and bipolar cells, to the lateral geniculate body through the optic nerve, optic tract, optic chiasm, and optic radiation.[1] These cells are affected by several pathological conditions, including optic neuropathies and glaucoma.[2] Particularly, glaucoma, which is characterized by progressive death of RGCs, is the leading cause of irreversible blindness and more than 70 million people suffer from glaucoma worldwide.[3,4] Although medications and surgery for glaucoma are available, 10% of glaucoma patients still lose their vision despite receiving appropriate treatment.[5] The loss of RGCs has been also implicated in genetic optic neuropathy, such as Leber's hereditary optic neuropathy and dominant optic atrophy.[6] Both optic neuropathies show bilateral and aggressive loss of vision in younger patients, and no promising treatment has been developed for these conditions.

Recent advances in stem cell biology have indicated that stem cells can be used as an alternative therapy for such incurable RGC-related diseases.[7] Particularly, human pluripotent stem cells (hPSCs) derived from patients with genetic defects are an excellent in vitro model for studying the pathophysiology of these diseases and developing new drugs. To develop treatment strategies employing stem cell technology, an efficient differentiation method for RGCs is required. Several methods for generating RGCs from hPSCs (embryonic stem cells [ESCs] and induced pluripotent stem cells [iPSCs]) have been reported, and one group has applied their method for modeling an RGC disease with inherent genetic alterations.[8–13]

Differentiation methods for retinal cells often involve three-dimensional (3D) culture of PSCs to allow for self-organization of the primordial structure of the eye.[14,15] These structures include optic vesicles and optic cups, which eventually give rise to most retinal lineages, including photoreceptors, retinal pigmented epithelia (RPE), and RGCs within the structure. Under such culture conditions, various retinal cell types arise and are arranged in a proper retinal layer; however, the large-scale

culture or enrichment of particular retinal cells (i.e., RGCs) may be limited. Other studies have employed an adherent culture platform either from the beginning or following 3D culture; however, because of the heterogeneity of the cell population and low yield of RGCs in culture, an enrichment step was still required.[9,12] Insufficient specification of a specific retinal cell type may result from using methods that rely on the inherent differentiation program of an individual hPSC line. Induction of retinal cells based on such methods is not always efficient for certain hPSC lines, particularly when some display an unfavorable propensity toward retinal fate.[16] Other studies attempted to specify RGCs by modulating the cellular signals involved in RGC development during neural differentiation from hPSCs.[10,13,17] This approach resulted in substantial technical advances; however, modulation of cellular signals occurs in a less-defined manner via treatment with a cocktail of chemicals, signaling molecules, and sometimes fetal bovine serum, thus resulting in a low yield of RGCs. Additionally, this unclearly defined cocktail makes it difficult to determine which signaling pathway and the extent of pathway modulation are required to maximize RGC differentiation.

To define the contribution of specific signal pathways to RGC development and thereby to optimize the differentiation of hPSCs toward RGCs, we dissected the process of RGC differentiation into three stages as in vivo: (1) eye field progenitors expressing a set of transcription factors (eye field transcription factors [EFTFs]), (2) RGC progenitors expressing MATH5, and (3) RGCs expressing BRN3B and ISLET1.[18–24] In each stage, the roles of several key signaling pathways in RGC differentiation were investigated using different concentrations and combinations of small molecules and peptide modulators. While monitoring the condition showing the highest yield of cells expressing stage-specific markers, we identified the signaling pathways that require modulation and level of modulation required for efficient generation of RGCs from hPSCs.

Methods

Culture of hPSCs and Differentiation of RGCs

Human ESCs (H9 [WA09, P35–50], WiCell, Madison, WI, USA) and human iPSCs derived from healthy subjects[25] were cultured on mitotically arrested mouse fibroblasts (STO, CRL-1503, American Type Culture Collection, Manassas, VA, USA) in human ESC medium composed of DMEM/F12 medium (Invitrogen, Carlsbad, CA, USA) supplemented with 20% Knockout-Serum Replacement (Invitrogen), 1× nonessential amino acids (Invitrogen), 0.1 mM beta-mercaptoethanol (Sigma-Aldrich Corp., St. Louis, MO, USA), and 4 ng/mL basic fibroblast growth factor (bFGF, Peprotech, Rocky Hill, NJ, USA). To induce eye field progenitors, embryoid bodies (EBs) were cultured for 4 days in suspension with 5 μM dorsomorphin (DM; Calbiochem, La Jolla, CA, USA), 5 μM SB431542 (SB; Sigma-Aldrich Corp.), 0.5 to 1 μM XAV939 (XAV; Calbiochem), and 5 to 10 ng/mL insulin-like growth factor-1 (IGF-1; Peprotech) in human ESC medium without bFGF. After transferring the cells to Matrigel (BD Biosciences, San Jose, CA, USA)-coated dishes, EBs were cultured in N2 medium containing DMEM/F12 and 1× N2 (Gemini Bio-Products, West Sacramento, CA, USA) supplemented with 2 μL/mL insulin (Sigma-Aldrich Corp.), 1 μM XAV, and 10 to 60 ng/mL bFGF for an additional 4 days. Neural rosettes that appeared in the center of attached EB colonies were carefully isolated from the surrounding flat cells using pulled glass pipettes, and then small rosette clumps were seeded onto Matrigel-coated dishes after gentle trituration. These cells were then cultured in N2B27 medium containing DMEM/F12, 1× N2, and 1× B27 without vitamin A (Invitrogen) supplemented with 20 ng/mL bFGF. Upon reaching approximately 90% confluence, the cells were dissociated into single cells by incubation with Accutase (Millipore, Billerica, MA, USA) and re-plated onto new Matrigel-coated dishes in N2B27 medium. The culture medium was changed every day, and cells were passaged every 2 to 3 days for further expansion. For differentiation toward RGCs, cells were seeded onto poly-D-lysine (Sigma-Aldrich Corp.) and laminin (BD Biosciences)-coated dishes and cultured in N2B27 medium supplemented with 4 μM with *N*-(*N*-[3,5-difluorophenacetyl]-L-alanyl)-*S*-phenylglycine *t*-butyl ester (DAPT; Sigma-Aldrich Corp.) for 10 days. Brain-derived neurotrophic factor (BDNF; Peprotech) was added beginning on day 16 to improve the survival of neurons by the end of differentiation. A schematic process for RGC differentiation is shown in Supplementary Figure S1.

Quantitative Polymerase Chain Reaction

Total RNA was isolated using the Easy-Spin Total RNA Extraction Kit (iNtRON Biotechnology, Gyeonggi-Do, Korea), and cDNA was then synthesized from 1 μg total RNA using the PrimeScript RT Master Mix (Takara Bio, Shiga, Japan). Transcript levels were quantified by real-time RT-PCR assays using SYBR Premix Ex Taq (Takara Bio) and the CFX96 Real-Time System (Bio-Rad, Hercules, CA, USA). Ct values for each targeted gene were normalized according to β-actin expression, and the normalized expression levels of the targeted genes were compared to control samples using the comparative Ct method. Data are expressed as the mean relative expression ± standard error of the mean (SEM) from at least three independent experiments. Primers sequences are provided in Supplementary Table S1.

Immunocytochemistry Analysis

Cells fixed in 4% paraformaldehyde phosphate-buffered saline (PBS) were permeabilized with 0.1% Triton X-100-PBS solution for 10 minutes and then blocked with 2% bovine serum albumin in PBS for 1 hour at room temperature. Next, the cells were incubated with primary antibodies overnight at 4°C. The following primary antibodies were used in our study: SOX2, 1:200, Millipore [MAB4343]; PLZF, 1:50, Calbiochem [OP129L]; RX, 1:300, Abcam (Cambridge, UK) [ab23340]; PAX6, 1:100, DSHB (Iowa City, IA, USA) [pax6]; LHX2, 1:300, Santa Cruz Biotechnology (Dallas, TX, USA) [sc-19344]; MATH5, 1:500, Millipore [AB5694]; BRN3B, 1:200, Santa Cruz Biotechnology [sc-31989]; ISLET1, 1:200, Abcam [ab20670]; TUJ1, 1:1000, BioLegend (San Diego, CA, USA) [801201]; and NF-L, 1:200, Millipore [AB9568].

Appropriate fluorescence-tagged secondary antibodies (Molecular Probes, Eugene, OR, USA) were used for visualization. Cells were mounted in DAPI mounting medium (Vector Laboratories, Burlingame, CA, USA) and images were obtained using an IX71 microscope equipped with a DP71 digital camera (Olympus, Tokyo, Japan) or FSX100 all-in-one fluorescence microscope system (Olympus). Positively-labeled cells were counted manually by blinded examiners or using an image analysis program (MetaMorph version 7.17; Molecular Devices, Sunnyvale, CA, USA) with at least six randomly captured images from three independent experiments.

Time-Lapse Imaging for Axonal Transportation of Mitochondria

RGCs at day 40 of differentiation were labeled with Mitotracker Red CMXRos (Molecular Probes) according to the manufactur-

er's instructions and observed with an Eclipse Ti-U inverted microscope equipped with a DS-U3 camera and Intensilight C-HGFI (Nikon, Tokyo, Japan) under 400× magnification. Live imaging was performed for 30 seconds to 2 minutes at each region of interest, and time-lapse images were acquired every 7 seconds from the recorded video clips.

Electrophysiological Analysis

Electrophysiological examinations were performed with human ESC and iPSC-derived RGCs using the whole-cell patch clamp technique as reported previously.[26] Briefly, cultured cells were transferred into a bath mounted on a stage with an inverted microscope (IX-70, Olympus). Cells subjected to electrophysiological recording were identified by the morphological features of RGCs such as their medium-sized (15–25 μm in diameter) and oval-shaped soma with two or more intensively long processes.[27] The conventional whole-cell clamp was achieved by rupturing the patch membrane after forming a gigaseal. The bath solution (124 mM NaCl, 3 mM KCl, 1.25 mM KH_2PO_4, 2.5 mM $MgSO_4$, 3.4 mM $CaCl_2$, 26 mM $NaHCO_3$, 10 mM glucose [pH 7.4]) was perfused at 1.5 mL/min and continuously gassed with 95% O_2 and 5% CO_2. The standard pipette solution for the whole-cell patch clamp contained 130 mM K-gluconate, 10 mM KCl, 8 mM NaCl, 2 mM MgATP, 0.5 mM GTP, 10 mM HEPES, and 0.2 mM ethylene glycol tetraacetic acid (pH 7.2). The voltage and current recordings were performed at room temperature (22°C–25°C). Patch pipettes with a free-tip resistance of approximately 2 to 5 MΩ were connected to the head stage of the patch-clamp amplifier (Axopatch-700B, Molecular Devices). pCLAMP software version 10.2 and Digidata-1440A (Molecular Devices) were used to acquire data and apply command pulses. AgCl reference electrodes were connected to the bath via a 1.5% agar bridge containing 3 M KCl. Voltage and current traces were stored and analyzed using Clampfit version 10.2 and Origin version 8.0 (OriginLab Corp., Northampton, MA, USA). Currents were sampled at 5 kHz. All data were low-pass filtered at 1 kHz. Depolarizing currents to induce action potentials were injected at 0.01 mA for 500 ms. All data are presented as the mean ± SEM.

Statistical Analysis

Data are shown as the mean ± SEM of at least three independent replicates. Data were analyzed by two-tailed Student's *t* tests or analysis of variance when two or more groups were involved. Statistical analyses were performed using SPSS version 23 software (SPSS, Inc., Chicago, IL, USA).

Results

To initiate retinal differentiation from human ESCs, we induced the neuroectoderm by simultaneously inhibiting both bone morphogenic protein (BMP) and transforming growth factor beta (TGFβ) signals using two small molecules, DM and SB, as previously described.[28] An attachment culture of EBs pre-exposed to these small molecules for 4 days generated colonies with neural rosette structures (Supplementary Figs. S2A–C). Most cells in the structure were positive for SOX2 and PLZF, which are markers of neural rosette cells (Supplementary Figs. S2D, S2E), confirming robust neural induction. Thus, we utilized this method as a basis for generating eye field progenitors.

Inhibition of Wnt in Combination With Activation of IGF Induces Eye Field Progenitors

The eye field is first specified in the anterior neural plate as the eye primordium, which eventually forms the visible optic cup via evagination of the diencephalic wall.[19] This region can be identified by specific expression of EFTFs, such as Pax6, Rx, Six3, and Lhx2.[19] Previous studies showed that the anterior fate of the neuroectoderm is greatly enhanced upon inhibition of canonical Wnt signaling.[29] Thus, we first tested whether Wnt signal inhibition facilitates anteriorization of the neuroectoderm as well as eye field specification. To this end, we employed XAV, a potent tankyrase inhibitor, to inhibit canonical Wnt signaling.[30] We treated EBs with 1 μM XAV for 4 days in the presence of small molecule inhibitors of BMP and TGFβ. Quantitative gene expression analysis of neuroectoderm markers and the anteroposterior axis revealed that XAV treatment significantly upregulated the expression of a forebrain marker, *BF1* (also known as *FOXG1*), whereas such treatment downregulated expression of mid- and hindbrain markers, *EN1* and *GBX2*, compared to levels in the DM and SB-treated control group (Fig. 1A). The expression level of *SOX1*, a pan-neural marker gene, was not significantly different in XAV-treated cells compared to in a control (Fig. 1A). We next examined whether Wnt inhibition promotes the expression of EFTFs. As shown in Figure 1B, treatment of EB-stage cells with 0.5 to 1 μM XAV for 4 days significantly enhanced the expression of EFTFs. XAV treatment with 1.0 μM did not significantly increase *PAX6* expression compared to the control condition (DM and SB only), while 0.5 μM of XAV did increase *PAX6* expression. However, the fold-increase in *PAX6* by XAV treatment was marginal at both concentrations (1.56-fold at 0.5 μM and 1.13-fold at 1.0 μM), and upregulation of *RX* and *SIX3* by XAV treatment was robust at 1.0 μM and displayed a clear dosage-dependency (4.11- and 3.67-fold at 0.5 μM and 18.46- and 12.95-fold at 1.0 μM). Therefore, we used 1.0 μM XAV for retinal induction.

Based on a previous study that reported IGF-1 as a positive regulator of eye and head induction in *Xenopus*,[31] we examined whether IGF-1 treatment enhances the expression of anterior markers and/or EFTFs. When EBs were exposed to IGF-1 in the presence of DM and SB for 4 days, *BF1* and *OTX2* (another anterior marker) were slightly but significantly upregulated by 1.42- and 1.38-fold, respectively, while *GBX2* was downregulated by 2.32-fold with no significant change in *EN1* expression compared to in DM- and SB-treated cells (Fig. 1C). The fold-change in anteroposterior marker expression following IGF-1 treatment was not as robust as that following XAV treatment; however, IGF-1 treatment significantly increased the expression of all EFTFs tested (2.2- and 2.4-fold for *PAX6*, 12.7- and 17.6-fold for *RX*, 2.3- and 2.1-fold for *SIX3*, and 2.5- and 2.0-fold for *LHX2* by 5 and 10 ng/mL of IGF-1, respectively) and showed a clear dose-dependent effect on *RX* (Fig. 1D). Thus, our results indicate that IGF-1 treatment imparts eye field identity to differentiating neural progenitors and induces anteriorization.

Because both IGF-1 and XAV treatment promoted anteriorization and eye field fate, we tested whether co-treatment of these cells with IGF-1 and XAV would have an additive effect on eye field specification. Addition of 10 ng/mL IGF-1 in combination with DM, SB, and 1 μM XAV to the EB culture increased the expression of *RX* and *SIX3* by 32.5- and 30.2-fold compared to expression in EB cultures treated with DM and SB only (Fig. 1E). These expression levels were 1.8- and 2.3-fold greater than those in DM, SB, and XAV-treated EB cultures (Fig. 1B versus Fig. 1E). The expression of *PAX6* was not significantly increased, possibly because PAX6 expression in EB cultures already peaked by co-treatment with DM and SB.[32] Together, our data suggest that Wnt inhibition and IGF activation cooperatively promote eye field fate during neural induction of human ESCs.

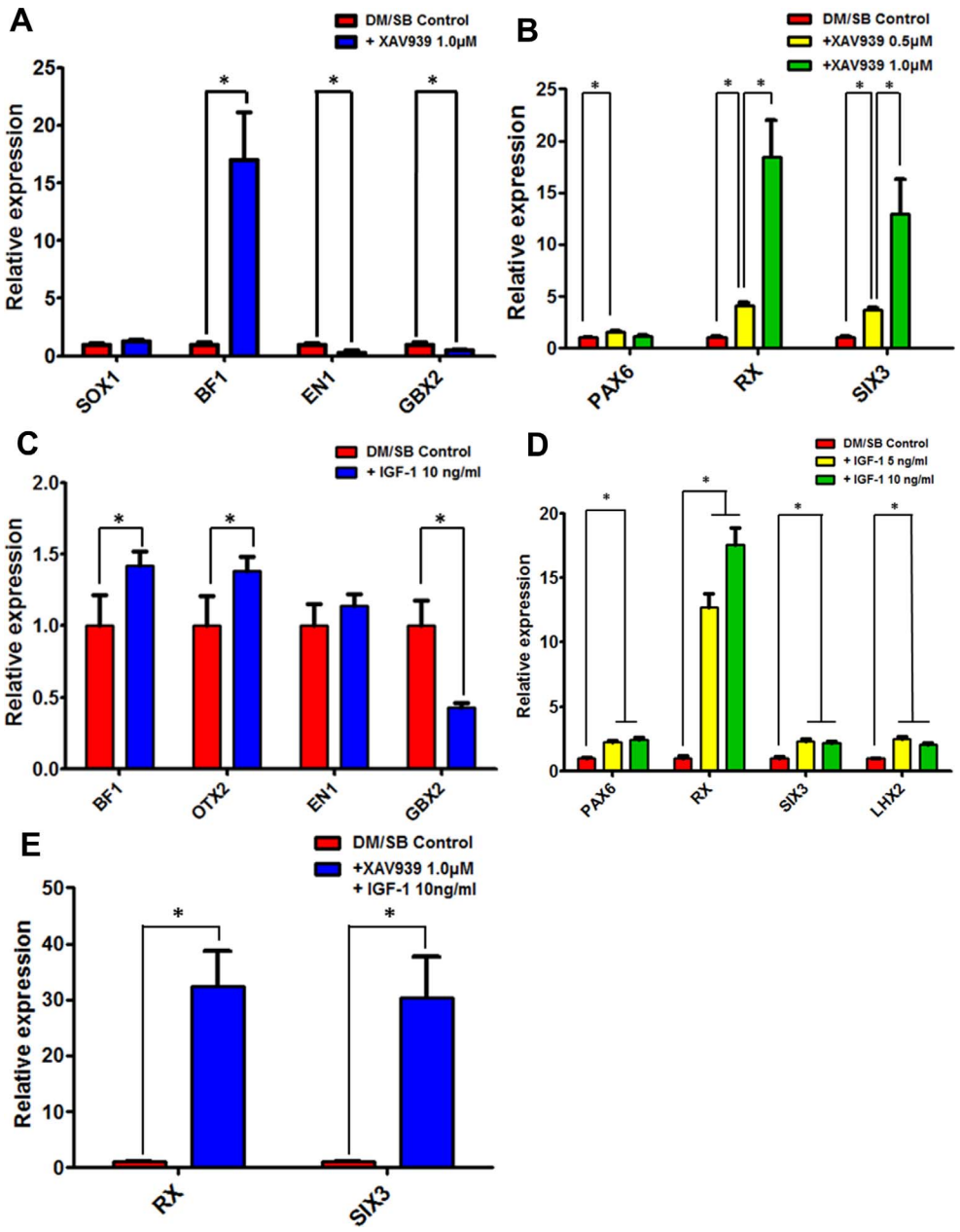

FIGURE 1. Modulation of Wnt and IGF signals promoted anteriorization and eye field specification. (**A**) Wnt inhibition anteriorized the cells in neural differentiation of human ESCs. (**B**) Wnt inhibition increased the expression of EFTFs, particularly *RX* and *SIX3*, in a dose-dependent manner. (**C**) IGF-1 showed anteriorizing effect in neural induction of human ESCs. (**D**) IGF-1 significantly upregulated the expression of EFTFs. (**E**) Wnt inhibition and IGF activation cooperatively increased the expression of *RX* and *SIX3*. All data are presented as the mean ± SEM. Significant differences are indicated as $^{*}P < 0.05$.

Enrichment of Eye Field Progenitors by Treatment With bFGF and Mechanical Isolation of Rosette Structure

To further investigate the effect of modulating additional signaling pathway(s) on eye field specification, we transferred EBs onto Matrigel-coated dishes after culture in the presence of DM, SB, XAV, and IGF-1 for 4 days. Various stimuli, including retinoic acid, acidic FGF, bFGF, and purine agonist were tested in the adherent culture. None of the stimulants, such as the purine agonist 2-methylthioadenosine diphosphate trisodium, all-trans retinoic acid, and acidic FGF, significantly increased the expression of *RX* and *SIX3* when added to cultures for 4 days (data not shown). However, treatment with a high dose of bFGF (60 ng/mL) upregulated the expression of both *RX* and *SIX3* by 4.6- and 3.9-fold, respectively, compared to nontreated cells (Fig. 2A). In zebrafish, Fgf-8 regulates axial patterning of the prospective neural retina,[33] and Fgf-3 and Fgf-19 regulate Hedgehog signaling, which is required for differentiation of the vertebrate retina.[34,35] Given that bFGF can bind to several FGF receptors that bind the retina-inducing FGFs mentioned above (i.e., FGFR3c, FGFR2c, and FGFR1b) with different affinities,[36] it is possible that only high concentrations of bFGF are effective for eye field specification.

Morphological identification has been employed to enrich RGCs from a heterogeneous population.[10] In adherent cultures, the colonies of attached EBs were a heterogeneous mixture of neural rosette cells and surrounding nonrosette-

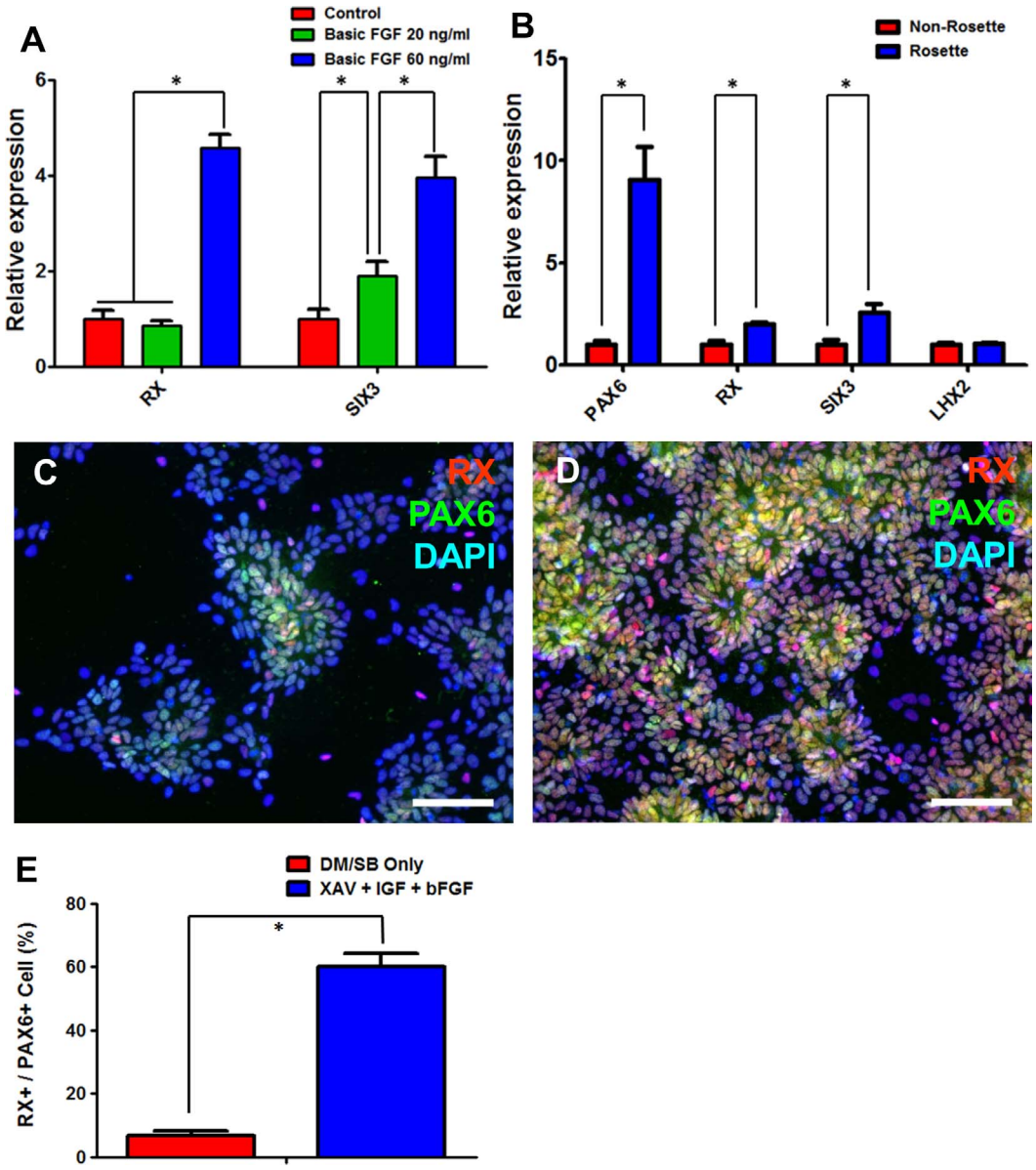

Figure 2. Treatment with bFGF and isolation of neural rosette enriched eye field progenitors. (**A**) Quantitative RT-PCR analysis showed that treatment with a high concentration (60 ng/mL) of bFGF significantly upregulated *RX* and *SIX3* compared to the untreated control group. (**B**) Expression of EFTFs (*PAX6*, *RX*, *SIX3*, but not *LHX2*) was higher in neural rosette clusters than in nonneural rosette cells. (**C–E**) RX and PAX6-double positive cells were more prevalent (up to 60% of total cells) in neural rosette clusters isolated from neural culture treated with DM, SB, XAV, IGF-1, and bFGF than in neural cells induced by treatment with DM and SM. (**C**) and (**D**) show representative immunofluorescent images of each group, and (**E**) shows the results of quantitative analysis of RX and PAX6 double-positive cells in the cultures. *Scale bar*: 100 µm. Data are presented as the mean ± SEM. Significant differences are indicated as $^*P < 0.05$.

type cells, which could be distinguished morphologically (Supplementary Figs. S2B, S2C). To determine whether the two cell types differ in their potential for RGC differentiation, we assessed EFTF gene expression following dissection of the two cell types under a microscope. Relative gene expression analysis clearly showed higher expression of EFTFs in the rosette group than in the nonrosette group (Fig. 2B). Moreover, neural rosette cells obtained from eye field-inducing conditions were strongly labeled with antibodies against PAX6 and RX, and approximately 60% of the total cells coexpressed PAX6 and RX under these conditions, while only 6.7% coexpression was observed under control conditions with DM and SB treatment only (Figs. 2C–E). Considering that nonneural rosette cells that appeared around the neural rosette clumps after neural induction were mainly composed of neural crest cells[37] and that neural crest cells never follow the RGC lineage, it was not surprising that isolation of neural rosette enriches eye-field progenitors. The neural rosette cells at this stage were cryopreservable and propagated without changing their characteristics after thawing (data not shown). Given the high proportion of cells with dual-immunoreactivity for PAX6 and RX, we referred to cells at this stage as eye field progenitors and used these cells for further RGC differentiation.

Notch Signal Inhibition Induces RGCs From Eye Field Progenitors via MATH5-Positive RGC Progenitor Stage

Cell cycle exit can be induced by Notch signal inhibition.[38] Additionally, Notch activity is downregulated just prior to RGC differentiation in intact developing chick retinas[39] and Notch signaling appears to control the stage-dependent phenotypic potential of retinal progenitors.[40] Because RGCs are first generated from retinal progenitors by mitotic exit during retina development,[41] we predicted that RGCs would accumulate following early Notch signal inhibition. To test this hypothesis, we treated the eye field progenitors with DAPT, a small molecular inhibitor of Notch signaling. Morphological examination revealed that oval-shaped cell bodies with extended bipolar dendrites were prominent 1 week after DAPT treatment (Fig. 3A), indicating facilitation of neuronal differentiation. Immunocytochemical analysis for the RGC precursor marker MATH5 (also known as ATOH7) and pan-neuronal marker TUJ1 revealed that up to 90% ± 2% of total cells were double-positive for these markers 8 days after beginning DAPT treatment (at day 20; Fig. 3B). Because of the high percentage of MATH5-positive cells observed, we referred to this cell stage as MATH5-positive RGC progenitors.

For terminal maturation, the MATH5-positive RGC progenitors were further cultured in differentiation medium supplemented with BDNF for 3 to 4 weeks. At day 26 of differentiation, quantitative gene expression analysis showed that MATH5-positive RGC progenitors cultured under maturation conditions expressed significantly higher levels of RGC markers, including *BRN3B*, and the cell-surface glycoprotein *THY1*[42] than neural cells differentiated under non-RGC-inducing conditions (Figs. 3C, 3D). At day 40 of differentiation, numerous cells formed small cell clusters, intensively networking with each other via long neuronal processes (Fig. 3E). Immunocytochemistry with antibodies against BRN3B and ISLET1 followed by quantitative analysis revealed that 51.8% ± 7.9% of cells were BRN3B-positive, 74.7% ± 5.5% of cells were ISLET1-positive, and 44.6% ± 7.3% of cells were positive for both markers (Fig. 3F).

We then examined the time-course of expression of the following markers representative of retinal lineages: RPE marker *MITF*,[43] photoreceptor marker *CRX*,[44] amacrine cell marker *BARHL2*,[45] horizontal cell marker *PROX1*,[46] Müller cell marker *GLUL*,[47] retinal progenitor and bipolar cell marker *CHX10* (also known as *VSX-2*),[48] and RGC markers *BRN3B* and *γ-synuclein* (*SNCG*).[49] The relative expression of markers in cells cultured under RGC-inducing conditions normalized to expression in cells grown under control conditions revealed robust upregulation of all EFTFs (*SIX3*, *RX*, and *LHX2*) in the early stage (days 4–8), followed by delayed upregulation of the retinal progenitor marker CHX10 at day 12 (Fig. 3G). Markers for RGCs (*MATH5, BRN3B*, and *SNCG*) were highly upregulated at later stages of differentiation (at days 19–40), suggesting that RGC differentiation proceeded via a normal developmental trajectory as observed for RGCs in developing retinas.[19] Interestingly, only transient upregulation of MITF and PROX1 expression was observed at day 12 and 19, respectively, and upregulation of BARHL2 was particularly high at day 19 (Fig. 3G). No significant change in the expression of CRX was observed, indicating that the differentiation of photoreceptors was negligible. These results demonstrate that other retinal lineage cells (e.g., RPE, horizontal cells, and amacrine cells) arise together with RGCs under the conditions used in this study. Nonetheless, the high proportion of BRN3B and ISLET1 double-positive cells and timely upregulation of various RGC makers reminiscent of in vivo RGC development suggest that our differentiation strategy involving defined modulation of cellular signals is efficient for inducing RGCs from human ESCs.

Functionality of RGCs Derived From hPSCs

To determine whether the human ESC-derived RGCs were functionally active, we examined their electrophysiological properties at day 40 of differentiation. In all recordings, the subject cells were carefully selected based on the morphological features of RGCs[27] (Fig. 4A) as described in the Methods section, although such an approach is often accompanied by a risk of off-targeting. In voltage-clamp mode, most neurons examined showed fast inward sodium currents and an outward rectifying potassium current (Fig. 4B). In current-clamp mode, the resting membrane potential was −30.4 ± 1.9 mV and amplitude of the first action potential was 37.7 ± 2.7 mV in human ESC-derived neurons (n = 12) (Supplementary Table S2). Human ESC-derived neurons (70.6%, n = 12/17) consistently produced trains of action potentials in response to the depolarizing current injection under the current-clamp mode (Fig. 4C). We also observed spontaneous firings for a few neurons (Fig. 4D), indicating that neurons prepared using our system were electrophysiologically active.

The extensive projection of neuronal processes also prompted us to examine whether RGCs express neurofilament (NF) proteins using immunocytochemistry (Figs. 4E–F). Immunoreactivity of the NF component, neurofilament-light (NF-L), was strong on neuronal processes emanating from the cell cluster with BRN3B-immunoreactivity (Fig. 4E). Cells in less dense areas clearly exhibited dual immunoreactivity for NF-L and BRN3B and bipolar morphology (Fig. 4F). Given the role of NF in action potential transmission,[50] intensive expression of an NF component further supports the functionality of the differentiated cells as RGCs.

Strong expression of an NF component on its axons led us to examine whether the RGCs were capable of axonal transportation of mitochondria, which is one of the functional characteristics of RGCs. As shown in Figure 4G and the Supplementary Video, time-lapse imaging analysis using Mitotracker as a tracer of mitochondria clearly revealed mitochondrial transport along a neuronal axon. Even within a relatively short time frame (30 seconds–2 minutes), numerous clusters of mitochondria were transported bi-directionally with frequent pausing. Taken together, our data strongly suggest that the RGCs differentiated under our defined culture conditions were functionally active.

Finally, we tested the robustness of our method by generating RGCs from human iPSCs. Differentiation of human iPSCs by our RGC protocol produced RX and PAX6 double-positive cells at comparable efficiency in the eye field progenitor stage (day 12; Fig. 5A), and more than 90% of cells were positive for MATH5 and TUJ1 at day 20 (Fig. 5B). Further neuronal maturation following DAPT treatment generated terminally differentiated RGCs expressing BRN3B, ISLET1, and TUJ1 (Figs. 5C, 5D). Human iPSC-derived RGCs showed electrophysiological properties comparable to those of human ESC-derived RGCs (Figs. 5E–G, Supplementary Table S2). Most (80%, n = 16/20) consistently produced trains of action potentials in response to depolarizing current injection under the current-clamp mode (Fig. 5G), and a few neurons spontaneously fired action potentials (Fig. 5H), indicating that iPSC-derived neurons prepared using our system were electrophysiologically active.

Investigative Ophthalmology & Visual Science

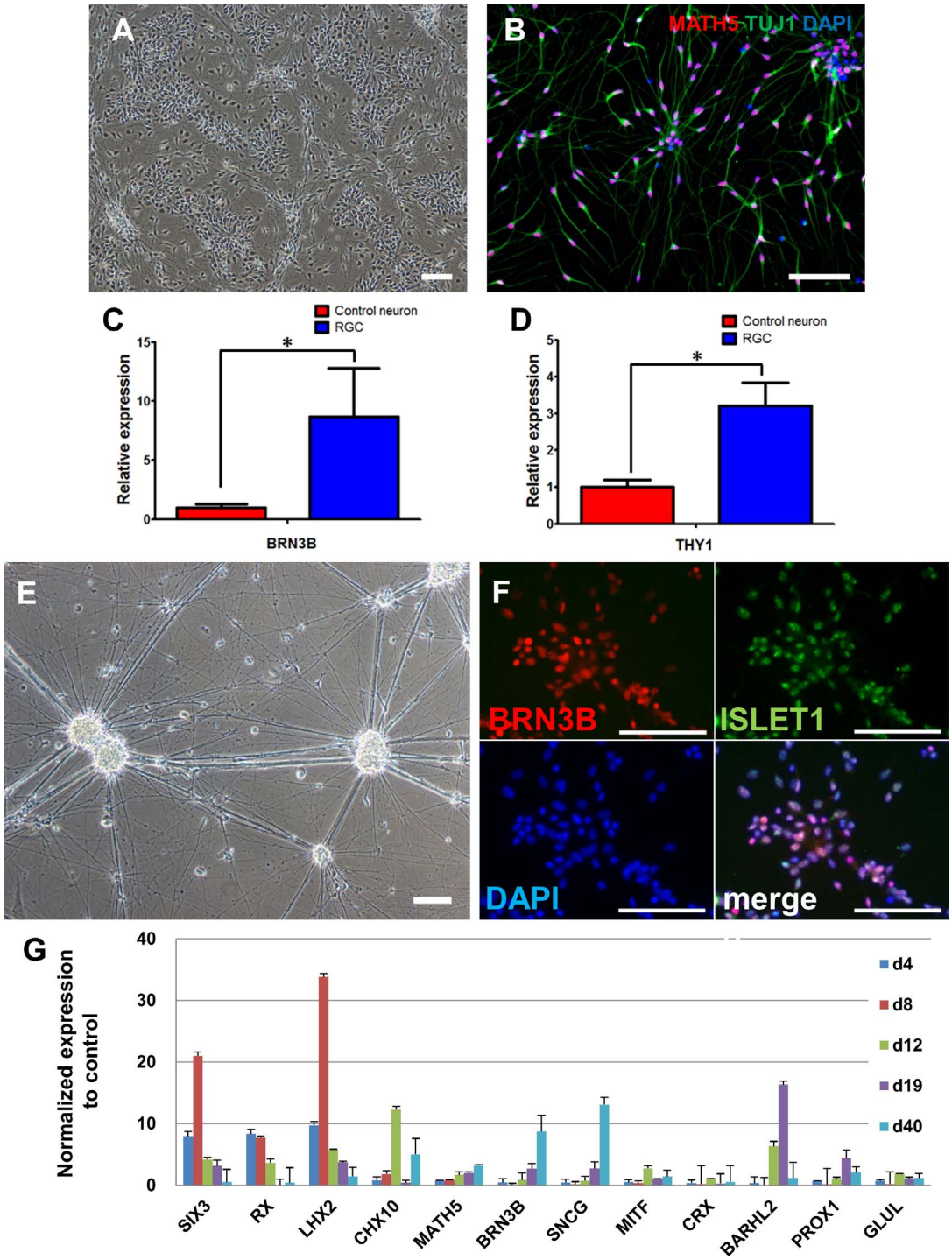

Figure 3. Notch inhibition facilitated differentiation of RGCs from eye field progenitors. (**A**) Representative bright-field image of RGC progenitors differentiating under Notch inhibition. (**B**) Immunofluorescent image showing that most differentiating cells coexpressed MATH5 and TUJ1. (**C**, **D**) Quantitative RT-PCR analysis at day 26 of differentiation showing significant upregulation of RGC markers ([**C**] for *BRN3B* and [**D**] for *THY1*) under RGC-induction conditions. (**E**) Representative image of 40-day-old neurons differentiating under RGC-inducing conditions. (**F**) Coexpression of BRN3B and ISLET1 in 40-day-old neurons differentiating under RGC-inducing conditions. (**G**) Time-course expression of retinal markers during RGC differentiation. *Bars* in the graph represent the relative expression of each marker in cells differentiating under RGC-inducing conditions normalized to those cultured under control conditions without RGC-inducing factors (XAV, IGF-1, and bFGF). *Scale bar*: 100 µm. Data are presented as the mean ± SEM. Significant differences indicated as $^*P < 0.05$.

Discussion

Our study presents a rapid, yet highly efficient, differentiation paradigm for generating RCGs from hPSCs. Fine modulation of the Wnt, IGF, and FGF signaling pathways, along with mechanical isolation of neural rosette clusters, generated an enriched cell population highly committed to retinal fate. Precocious cell cycle exit driven by Notch inhibition facilitated

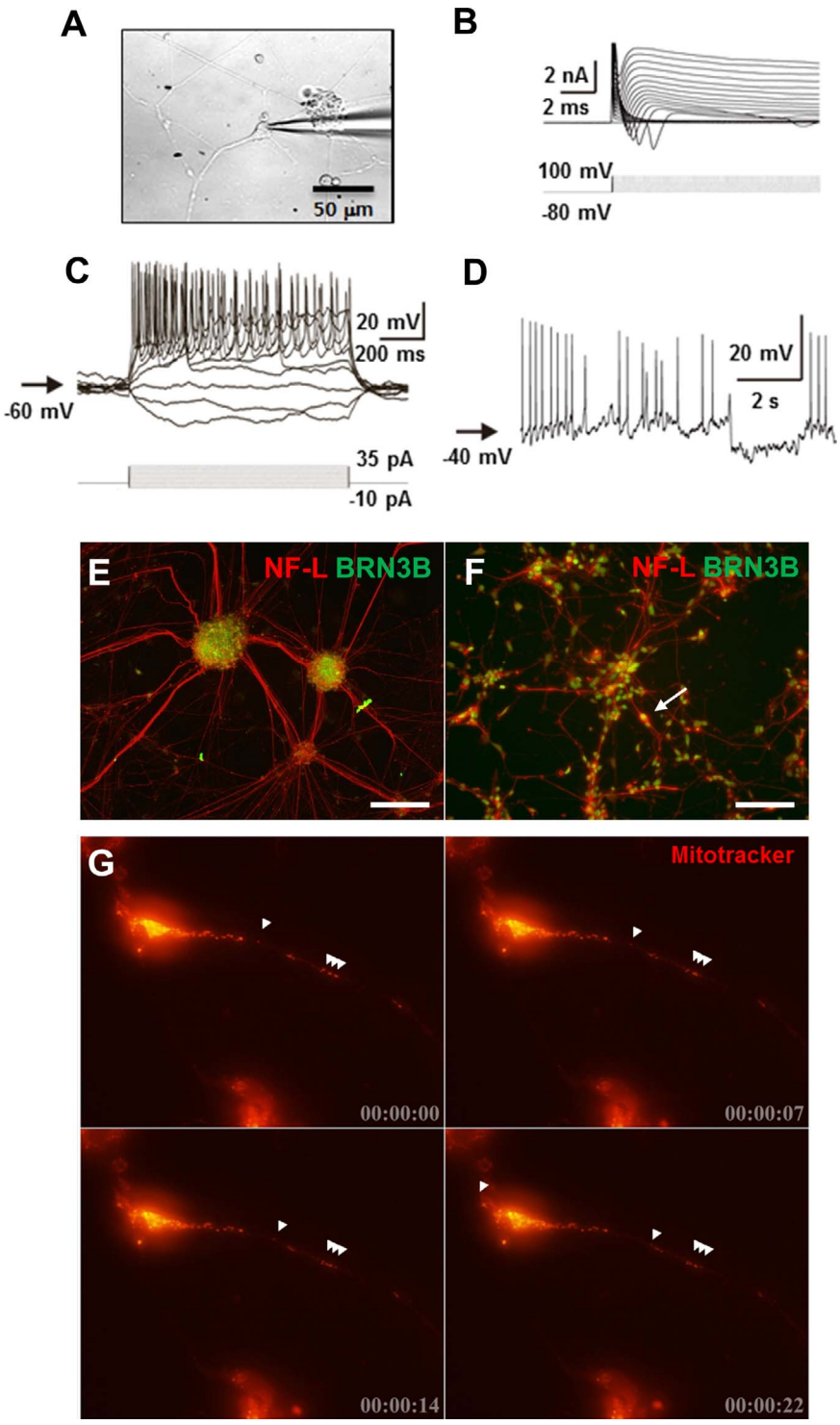

Figure 4. Functional assessment of differentiated RGCs from human ESCs. (**A**) Representative image of glass electrodes approaching neurons for patch-clamp recording. (**B**) Representative current traces (*upper panels*) recorded in voltage-clamp mode. Cells were depolarized by voltage steps from −80 to +100 mV in 10-mV increments (*lower panels*). (**C**) Voltage responses evoked by current steps (−10 to +35 pA in 5-pA increments, *lower panel*). (**D**) Spontaneous action potentials recorded in human ESC-derived RGCs. The *arrow* indicates membrane potentials. (**E**–**F**) Immunofluorescent images of neuronal cells coexpressing BRN3B and NF-L. The *arrow* in panel (**F**) indicates an RGC with co-immunoreactivity for BRN3B and NF-L. (**G**) Time-lapse images of Mitotracker-labeled neurons. Images were acquired under 400× magnification. *Arrowheads* follow the movement of a mitochondria cluster labeled by the tracer. *Scale bar*: 100 µm.

differentiation of these cells toward functional RGCs. As a result, we obtained MATH5-positive cells at more than 90% efficiency by day 20. Subsequent neuronal maturation generated BRN3B and ISLET1 double-positive RGCs at approximately 45% efficiency by day 40, which is the highest yield of BRN3B and ISLET1 double-positive cells reported from hPSCs without using cell sorting (Table). Most importantly, the differentiated RGCs exhibited characteristics of functional RGCs, including

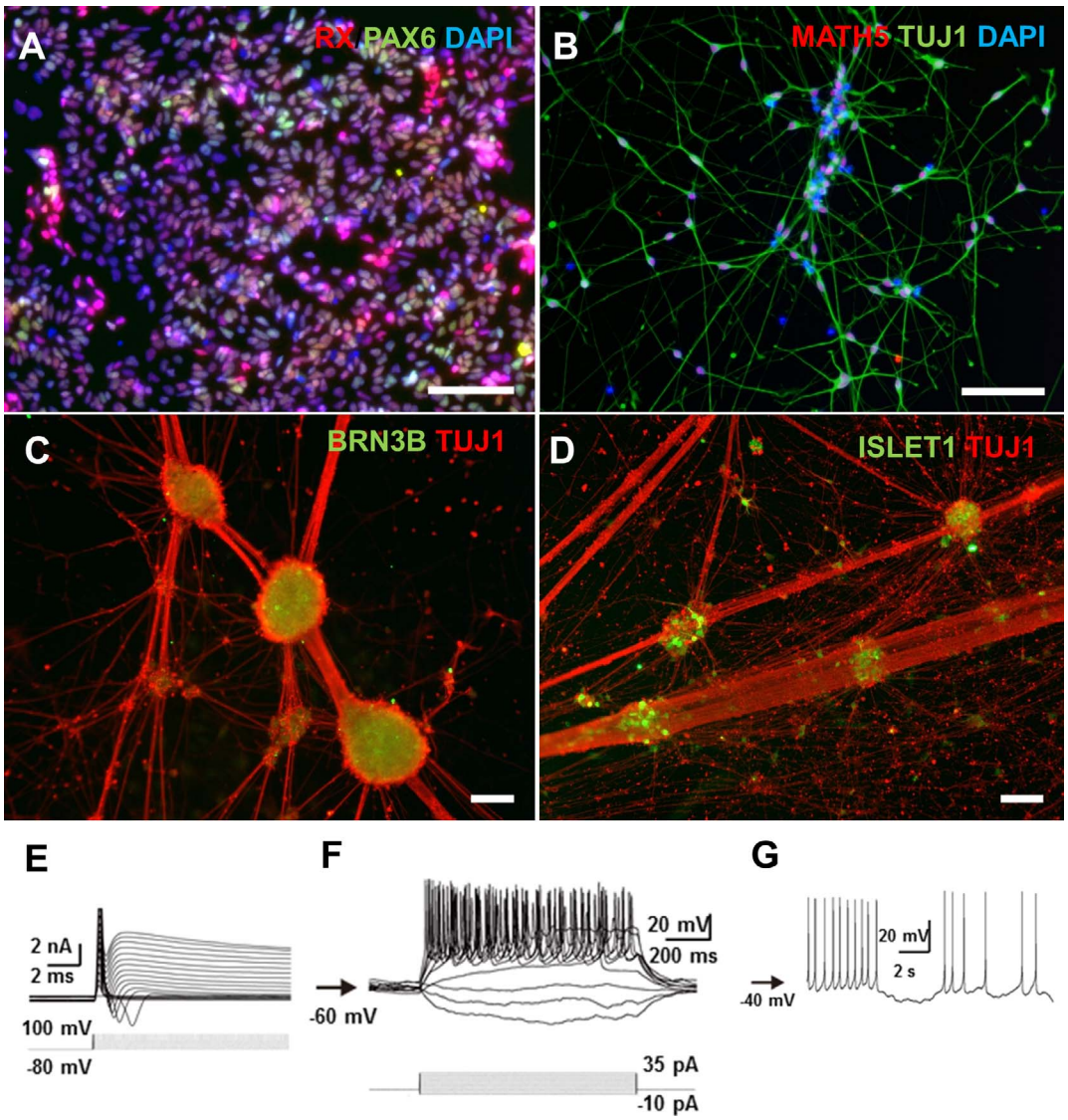

FIGURE 5. Generation of RGCs from human iPSCs. (**A**) Immunofluorescent image of human iPSC-derived neural cells coexpressing RX and PAX6 at the eye field progenitor stage. (**B**) Human iPSCs were differentiated to MATH5 and TUJ1 double-positive cells on day 20 at a comparable efficiency to human ESCs. (**C**, **D**) After neuronal maturation (at day 40), human iPSC-derived neurons clustered intensively extending neuronal processes to each other and showed strong immunoreactivity of BRN3B (**C**) and ISLET1 (**D**). (**E**) Representative current traces recorded in voltage-clamp mode. (**F**) Trains of action potentials evoked by current steps (−10 to +35 pA in 5-pA increments, *lower panel*). (**G**) Spontaneous action potentials recorded in human iPSC-derived RGCs. The *arrow* indicates membrane potentials. *Scale bars*: 100 μm.

generation of action potentials, expression of microfilament components, and axonal transportation of mitochondria.

The eye field firstly appears in the medial anterior neural plate of the human embryo at Carnegie stage 10 (4 weeks after gestation),[18] in which EFTFs are highly expressed, constituting a regulatory network for eye development.[19] This region forms the optic vesicle, then optic cup, and eventually undergoes retinal differentiation for following 2 weeks or more. RGCs are the first being born in developing neural retina.[20] Math5 is known to be required for commitment to RGCs and optic nerve formation, and its expression is primarily detected in embryonic day 11.5 mouse embryos (approximately equivalent to 5 weeks after gestation in human).[21,22] The Math5 gene is also known to function upstream of Brn3s to promote RGC development,[23] which occurs at embryonic days 11.5 to 12.5 in mice (approximately at 5–5.5 weeks in human), and Brn3 expression continues until embryonic day 15.5 (8 weeks in human), when most RGCs are generated.[24]

Our differentiation method generates eye-field progenitors from human ESCs in 8 days. Because ES cells are derived from the blastocyst, a 5- to 6-day-old embryo,[51] our method only required 2 weeks to differentiate the eye-field progenitors, which is 2 weeks earlier than expected in the normal developmental process. The efficient conditions used for neural induction by treatment with DM and SB in conjunction with promoting anteriorization (inhibition of WNT signal) and proretinal signaling (IGF-1) appeared to have increased the rate of retinal development. Thereafter, differentiation of MATH5-positive progenitors and BRN3-positive neurons from eye-field progenitors was facilitated by Notch signal inhibition, as the respective cells defined by the markers dominated the population earlier than in the developmental time course.

Despite our optimization efforts, the fates of more than half of the differentiated cells remained unclear. Considering the highly enriched eye field progenitor and RGC progenitor populations, the unidentified cells were likely retinal progen-

Table. Comparison Between Our Method and Recently Published Protocols for Differentiation of RGCs From hPSCs

Cell Type	Modulated Signals	RGC Marker	Yield	Functional Assays	Time Required	Similarity	Difference	Reference Number
hPSC	Dorsomorphin and SB431542 (dual SMAD inhibitors), XAV939 (Wnt inhibitor), IGF-1, bFGF, DAPT (Notch inhibitor)	BRN3B, ISL1, NF-L	~45%	Action potentials, Cytoskeleton in axons, Axonal transport	40 d	–	–	The present method
hPSC	DAPT (Notch inhibitor)	BRN3A, ISL1, SNCG, THY1	~22%	Action potentials, Excitatory postsynaptic currents	40 d	Notch inhibitor for early cell cycle exit	3D culture	8
hiPSC	IWR-1e (Wnt inhibitor), CHIR99021 (Wnt agonist), SAG (Shh agonist)	BRN3B, ISL1, SNCG, TAU, NF-L/M/H	N/A	Action potentials, Cytoskeleton in axons, Axonal transport	34 d	Wnt inhibition for eye-field	3D culture followed by adherent culture	9
hPSC	N/A	BRN3, ISL1, HUC/D, RBPMS, TAU	~36%	Action potentials, Cytoskeleton in axons	50 d	None	3D culture	10
hESC	Forskolin (Enhance cell survival)	BRN3B, BRN3A, THY1, RBPMS, PAX6, ISL1, NEUN, NF-H, TAU	~10%	Action potentials, Cytoskeleton in axons	40 d	None	Differentiation was carried out using only one condition	11
hESC	Noggin (BMP4 inhibitor), Dkk-1 (Wnt inhibitor), IGF-1, bFGF	THY1.1, BRN3A, HUC/D, NF-M	~77%	Action potentials, Cytoskeleton in axons, Axonal transport	45 d	Eye-field progenitors by Wnt inhibitor	Cell sorting mediated by THY1.1	13
hiPSC	Noggin, Dkk-1, IGF-1,Shh, FGF8, DAPT, Cyclopamine (Shh inhibitor) BDNF, NT4, CNTF, Forskolin, Y27632 (enhance cell survival)	BRN3/THY1	~26%	Action potentials, In vivo explant culture	36 d	Wnt inhibition for eye-field/Notch inhibitor for early cell cycle exit	Usage of Shh signal modulators	17

DKK-1, Dickkopf-related protein 1; CNTF, ciliary neurotrophic factor; NT4, neurotrophin4; Shh, Sonic Hedgehog.

itors still undergoing the maturation process or other retinal cells, such as horizontal cells and amacrine cells, as exemplified by their time-course gene expression (Fig. 3G). To further enhance the differentiation efficiency toward RGCs, modulation of other signals may be effective. For example, RA signaling plays an important role in retinal development.[52] RARα and RXRγ are expressed in the ganglion cell layer in the developing mouse retina,[53] and RA treatment for several days induces axonal growth in optic vesicles differentiated from human PSCs.[9] Although our early treatment with RA did not efficiently promote eye field specification, RA treatment in a later stage may be beneficial for maturation or axonal outgrowth of RGCs. The organic acid taurine (2-aminoethanesulfonic acid) may be another option because it is the most abundant molecule in the retina and has been implicated in the neuroprotection of RGCs.[54] Additionally, modulation of the TGFβ pathway may enhance the yield of differentiated RGCs because GDF11, a member of the TGFβ superfamily, is known to control the number of RGCs in the developing retina by controlling the proliferation of retinal progenitors expressing MATH5.[55] More recently, treatment with an adenylate cyclase activator was shown to promote eye field fate and RGC commitment in human ESCs.[12] Thus, additional fine modulation of such signals at the appropriate cellular stage may further improve the efficiency of RGC differentiation.

Although the heterogeneity issue requires further investigation, our study provides highly defined culture conditions for RGC differentiation, and these conditions can be manipulated to further increase efficiency and homogeneity. Given the applicability to human iPSCs, our method has remarkable potential for future applications, such as cell therapy, drug screening, and disease modeling for RGC-related diseases, including glaucoma and mitochondrial optic neuropathies.

Acknowledgments

Supported by the Bio & Medical Technology Development Program of the National Research Foundation (NRF) (2017M3A9B4042580), Basic Science Research Program of the NRF (2015R1D1A1A01056649) from the Ministry of Science and ICT, Korea Health Technology R&D Project from the Ministry of Health & Welfare (HI15C0916), and Korea University Grants (K1505391).

Disclosure: **J. Lee**, None; **S.-H. Choi**, None; **Y.-B. Kim**, None; **I. Jun**, None; **J.J. Sung**, None; **D.R. Lee**, None; **Y.I. Kim**, None; **M.S. Cho**, None; **S.H. Byeon**, None; **D.-S. Kim**, None; **D.-W. Kim**, None

References

1. Yu DY, Cringle SJ, Balaratnasingam C, Morgan WH, Yu PK, Su EN. Retinal ganglion cells: energetics, compartmentation, axonal transport, cytoskeletons and vulnerability. *Prog Retin Eye Res*. 2013;36:217–246.
2. Quigley HA, Broman AT. The number of people with glaucoma worldwide in 2010 and 2020. *Br J Ophthalmol*. 2006;90:262–267.
3. Weinreb RN, Aung T, Medeiros FA. The pathophysiology and treatment of glaucoma: a review. *JAMA*. 2014;311:1901–1911.
4. Weinreb RN, Leung CK, Crowston JG, et al. Primary open-angle glaucoma. *Nat Rev Dis Primers*. 2016;2:16067.
5. Medeiros FA, Alencar LM, Zangwill LM, Bowd C, Sample PA, Weinreb RN. Prediction of functional loss in glaucoma from progressive optic disc damage. *Arch Ophthalmol*. 2009;127:1250–1256.
6. Yu-Wai-Man P, Votruba M, Burte F, La Morgia C, Barboni P, Carelli V. A neurodegenerative perspective on mitochondrial optic neuropathies. *Acta Neuropathol*. 2016;132:789–806.
7. Chamling X, Sluch VM, Zack DJ. The potential of human stem cells for the study and treatment of glaucoma. *Invest Ophthalmol Vis Sci*. 2016;57:ORSFi1-ORSFi6.
8. Riazifar H, Jia Y, Chen J, Lynch G, Huang T. Chemically induced specification of retinal ganglion cells from human embryonic and induced pluripotent stem cells. *Stem Cells Transl Med*. 2014;3:424–432.
9. Tanaka T, Yokoi T, Tamalu F, Watanabe S, Nishina S, Azuma N. Generation of retinal ganglion cells with functional axons from human induced pluripotent stem cells. *Sci Rep*. 2015;5:8344.
10. Ohlemacher SK, Sridhar A, Xiao Y, et al. Stepwise differentiation of retinal ganglion cells from human pluripotent stem cells enables analysis of glaucomatous neurodegeneration. *Stem Cells*. 2016;34:1553–1562.
11. Maekawa Y, Onishi A, Matsushita K, et al. Optimized culture system to induce neurite outgrowth from retinal ganglion cells in three-dimensional retinal aggregates differentiated from mouse and human embryonic stem cells. *Curr Eye Res*. 2016;41:558–568.
12. Sluch VM, Davis CH, Ranganathan V, et al. Differentiation of human ESCs to retinal ganglion cells using a CRISPR engineered reporter cell line. *Sci Rep*. 2015;5:16595.
13. Gill KP, Hung SS, Sharov A, et al. Enriched retinal ganglion cells derived from human embryonic stem cells. *Sci Rep*. 2016;6:30552.
14. Eiraku M, Takata N, Ishibashi H, et al. Self-organizing optic-cup morphogenesis in three-dimensional culture. *Nature*. 2011;472:51–56.
15. Nakano T, Ando S, Takata N, et al. Self-formation of optic cups and storable stratified neural retina from human ESCs. *Cell Stem Cell*. 2012;10:771–785.
16. Meyer JS, Shearer RL, Capowski EE, et al. Modeling early retinal development with human embryonic and induced pluripotent stem cells. *Proc Natl Acad Sci U S A*. 2009;106:16698–16703.
17. Teotia P, Chopra DA, Dravid SM, et al. Generation of functional human retinal ganglion cells with target specificity from pluripotent stem cells by chemically defined recapitulation of developmental mechanism. *Stem Cells*. 2017;35:572–585.
18. Pearson AA. The development of the eyelids. Part I. External features. *J Anat*. 1980;130:33–42.
19. Heavner W, Pevny L. Eye development and retinogenesis. *Cold Spring Harb Perspect Biol*. 2012;4:a008391.
20. Graw J. Eye development. *Curr Top Dev Biol*. 2010;90:343–386.
21. Brown NL, Patel S, Brzezinski J, Glaser T. Math5 is required for retinal ganglion cell and optic nerve formation. *Development*. 2001;128:2497–2508.
22. Ko MS. Embryogenomics: developmental biology meets genomics. *Trends Biotechnol*. 2001;19:511–518.
23. Liu W, Mo Z, Xiang M. The Ath5 proneural genes function upstream of Brn3 POU domain transcription factor genes to promote retinal ganglion cell development. *Proc Natl Acad Sci U S A*. 2001;98:1649–1654.
24. Pan L, Yang Z, Feng L, Gan L. Functional equivalence of Brn3 POU-domain transcription factors in mouse retinal neurogenesis. *Development*. 2005;132:703–712.
25. Park C, Kweon J, Son JS, et al. Targeted inversion and reversion of the blood coagulation factor 8 gene in human iPS cells using TALENs. *Proc Natl Acad Sci U S A*. 2014;111:9253–9258.
26. Jun I, Cheng MH, Sim E, et al. Pore dilatation increases the bicarbonate permeability of CFTR, ANO1 and glycine receptor anion channels. *J Physiol*. 2016;594:2929–2955.
27. Peterson BB, Dacey DM. Morphology of human retinal ganglion cells with intraretinal axon collaterals. *Vis Neurosci*. 1998;15:377–387.
28. Kim DS, Lee JS, Leem JW, et al. Robust enhancement of neural differentiation from human ES and iPS cells regardless of their innate difference in differentiation propensity. *Stem Cell Rev*. 2010;6:270–281.
29. Maroof AM, Keros S, Tyson JA, et al. Directed differentiation and functional maturation of cortical interneurons from human embryonic stem cells. *Cell Stem Cell*. 2013;12:559–572.
30. Huang SM, Mishina YM, Liu S, et al. Tankyrase inhibition stabilizes axin and antagonizes Wnt signalling. *Nature*. 2009;461:614–620.
31. Pera EM, Wessely O, Li SY, De Robertis EM. Neural and head induction by insulin-like growth factor signals. *Dev Cell*. 2001;1:655–665.
32. Kim DS, Lee DR, Kim H, et al. Highly pure and expandable PSA-NCAM-positive neural precursors from human ESC and iPSC-derived neural rosettes. *PLoS One*. 2012;7:e39715.
33. Picker A, Brand M. Fgf signals from a novel signaling center determine axial patterning of the prospective neural retina. *Development*. 2005;132:4951–4962.
34. Vinothkumar S, Rastegar S, Takamiya M, Ertzer R, Strahle U. Sequential and cooperative action of Fgfs and Shh in the zebrafish retina. *Dev Biol*. 2008;314:200–214.
35. Esteve P, Bovolenta P. Secreted inducers in vertebrate eye development: more functions for old morphogens. *Curr Opin Neurobiol*. 2006;16:13–19.
36. Ornitz DM, Itoh N. The fibroblast growth factor signaling pathway. *Wiley Interdiscip Rev Dev Biol*. 2015;4:215–266.
37. Lee DR, Yoo J, Lee JS, et al. PSA-NCAM-negative neural crest cells emerging during neural induction of pluripotent stem cells cause mesodermal tumors and unwanted grafts. *Stem Cell Reports*. 2015;4:821–834.

38. Borghese L, Dolezalova D, Opitz T, et al. Inhibition of notch signaling in human embryonic stem cell-derived neural stem cells delays G1/S phase transition and accelerates neuronal differentiation in vitro and in vivo. *Stem Cells*. 2010;28:955–964.
39. Nelson BR, Gumuscu B, Hartman BH, Reh TA. Notch activity is downregulated just prior to retinal ganglion cell differentiation. *Dev Neurosci*. 2006;28:128–141.
40. James J, Das AV, Rahnenfuhrer J, Ahmad I. Cellular and molecular characterization of early and late retinal stem cells/progenitors: differential regulation of proliferation and context dependent role of Notch signaling. *J Neurobiol*. 2004;61:359–376.
41. Wallace VA. Concise review: making a retina–from the building blocks to clinical applications. *Stem Cells*. 2011;29:412–417.
42. Barnstable CJ, Drager UC. Thy-1 antigen: a ganglion cell specific marker in rodent retina. *Neuroscience*. 1984;11:847–855.
43. Capowski EE, Simonett JM, Clark EM, et al. Loss of MITF expression during human embryonic stem cell differentiation disrupts retinal pigment epithelium development and optic vesicle cell proliferation. *Hum Mol Genet*. 2014;23:6332–6344.
44. Swaroop A, Kim D, Forrest D. Transcriptional regulation of photoreceptor development and homeostasis in the mammalian retina. *Nat Rev Neurosci*. 2010;11:563–576.
45. Mo Z, Li S, Yang X, Xiang M. Role of the Barhl2 homeobox gene in the specification of glycinergic amacrine cells. *Development*. 2004;131:1607–1618.
46. Dyer MA, Livesey FJ, Cepko CL, Oliver G. Prox1 function controls progenitor cell proliferation and horizontal cell genesis in the mammalian retina. *Nat Genet*. 2003;34:53–58.
47. Jablonski M, Freeman NE, Orr WE, et al. Genetic pathways regulating glutamate levels in retinal Müller cells. *Neurochem Res*. 2011;36:594–603.
48. Green ES, Stubbs JL, Levine EM. Genetic rescue of cell number in a mouse model of microphthalmia: interactions between Chx10 and G1-phase cell cycle regulators. *Development*. 2003;130:539–552.
49. Surgucheva I, Weisman AD, Goldberg JL, Shnyra A, Surguchov A. Gamma-synuclein as a marker of retinal ganglion cells. *Mol Vis*. 2008;14:1540–1548.
50. Yuan A, Rao MV, Veeranna, Nixon RA. Neurofilaments and neurofilament proteins in health and disease. *Cold Spring Harb Perspect Biol*. 2017;9:a018309.
51. Pankratz MT, Li XJ, Lavaute TM, Lyons EA, Chen X, Zhang SC. Directed neural differentiation of human embryonic stem cells via an obligated primitive anterior stage. *Stem Cells*. 2007;25:1511–1520.
52. Cvekl A, Wang WL. Retinoic acid signaling in mammalian eye development. *Exp Eye Res*. 2009;89:280–291.
53. Mori M, Ghyselinck NB, Chambon P, Mark M. Systematic immunolocalization of retinoid receptors in developing and adult mouse eyes. *Invest Ophthalmol Vis Sci*. 2001;42:1312–1318.
54. Froger N, Moutsimilli L, Cadetti L, et al. Taurine: the comeback of a neutraceutical in the prevention of retinal degenerations. *Prog Retin Eye Res*. 2014;41:44–63.
55. Kim J, Wu HH, Lander AD, Lyons KM, Matzuk MM, Calof AL. GDF11 controls the timing of progenitor cell competence in developing retina. *Science*. 2005;308:1927–1930.

Supplementary Material

Supplementary Video. Live images of Mitotracker-labeled neurons. Live images using Mitotracker as a tracer of mitochondria demonstrated mitochondrial transport along a neuronal axon. Numerous clusters of mitochondria were transported bi-directionally with frequent pausing. Images were acquired under 400× magnification.

Investigative Ophthalmology & Visual Science